ARTICLE

Time-dependent Diffusion Coefficient and Conventional Diffusion Constant of Nanoparticles in Polymer Melts by Mode-coupling Theory

Xin-yu Lai, Nan-rong Zhao*

College of Chemistry, Sichuan University, Chengdu 610064, China

(Dated: Received on January 11, 2013; Accepted on February 1, 2013)

Time-dependent diffusion coefficient and conventional diffusion constant are calculated and analyzed to study diffusion of nanoparticles in polymer melts. A generalized Langevin equation is adopted to describe the diffusion dynamics. Mode-coupling theory is employed to calculate the memory kernel of friction. For simplicity, only microscopic terms arising from binary collision and coupling to the solvent density fluctuation are included in the formalism. The equilibrium structural information functions of the polymer nanocomposites required by mode-coupling theory are calculated on the basis of polymer reference interaction site model with Percus-Yevick closure. The effect of nanoparticle size and that of the polymer size are clarified explicitly. The structural functions, the friction kernel, as well as the diffusion coefficient show a rich variety with varying nanoparticle radius and polymer chain length. We find that for small nanoparticles or short chain polymers, the characteristic short time non-Markov diffusion dynamics becomes more prominent, and the diffusion coefficient takes longer time to approach asymptotically the conventional diffusion constant. This constant due to the microscopic contributions will decrease with the increase of nanoparticle size, while increase with polymer size. Furthermore, our result of diffusion constant from mode-coupling theory is compared with the value predicted from the Stokes-Einstein relation. It shows that the microscopic contributions to the diffusion constant are dominant for small nanoparticles or long chain polymers. Inversely, when nanonparticle is big, or polymer chain is short, the hydrodynamic contribution might play a significant role.

Key words: Time-dependent diffusion coefficient, Conventional diffusion coefficient, Polymer melts, Mode-coupling theory, Polymer reference interaction site model

I. INTRODUCTION

Understanding diffusion dynamics has been a central topic in solution chemistry and biochemistry due to its ubiquitous importance. In fact, many bimolecular reactions, such as the dissociation of a bimolecular complex [1], unfolding of a protein [2], or nanopore unzipping of DNA hairpins [3], are treated as a mutual diffusion on the potential of mean force along the reaction coordinate. In biophysics, the motion of proteins in crowded cellular environment is closely related to particle mobility in polymer matrix. Polymer nanocomposites, which involve nanoparticles dispersed in polymer melts and solutions, are of great importance both scientifically and for various technological applications [4, 5]. The diffusion of nanoparticles in complex fluids and polymer solutions is a problem of broad importance in materials science, cellular biophysics and even drug delivery [6, 7]. Up to now, a considerable amount of study has been devoted to investigating diffusion in solutions. Typical solutions include Lennard-Jones (LJ) liquids, as well as polymer nanocomposites. In particular, there are studies that analyzed the time-dependent diffusion coefficient and the transient diffusion dynamics in simple liquids on a basis of a mode-coupling theory (MCT) analysis [1]. Nevertheless, the theoretical formalism adopted in these works does not include the rich information of polymer chain structure as well as the intramolecular interaction between monomers, therefore it can not account for the effect of the polymer size, the nanoparticle/monomer size ratio and the interaction strength between monomers on the diffusion dynamics in polymer solutions. On the other hand, there are also studies [6, 10−13] that investigated the anomalous nanoparticle diffusion in polymer solutions and melts, based on either molecular dynamics (MD) simulation [6, 12] or theoretical analysis [10, 11], and even experimental observation [13]. However, they are limited to the study of conventional diffusion constant, which only deals with the long-time limit of the diffusion dynamics and is not capable of describing short time inertial motion. Furthermore, the short time non-Markov nature of the diffusion dynamics as well as the time-dependent diffusion coefficient has been less understood for these complex

*Author to whom correspondence should be addressed. E-mail: zhaonanr@scu.edu.cn

DOI:10.1063/1674-0068/26/02/163-171

solutions. The principal purpose of this work is therefore to describe a microscopic calculation of diffusion dynamics of nanoparticles in polymer melts from a theoretical point of view.

There are several approaches which have been widely used to study nanoparticle diffusion in polymer melts and solutions, including continuum models [14, 15], MCT [10, 11, 16, 17], MD simulations [6, 12], and so on. In the present work we will employ the mode-coupling theory to calculate the time-dependent friction, and adopt a generalized Langevin equation (GLE) incorporated the friction kernel from MCT to describe the diffusion dynamics of nanoparticles in polymer melts. The appealing approach of MCT may provide a clear microscopic picture of the dependence of friction on various parameters of polymer nanocomposites, such as nanoparticle size, polymer chain length, *etc.* Meanwhile, the GLE facilitates comprehensive examination on the dependence of diffusion coefficient on such parameters. By applying such formalism, not only the conventional diffusion constant, but also the time-dependent diffusion coefficient will be explicitly analyzed. Besides, the effect of the nanoparticle size and that of the polymer size to the diffusion dynamics will be investigated. Although there exists MCT formalism that takes into account entanglement effect in polymer melts, this effect is beyond the scope of our present work. Moreover, the hydrodynamic contribution to friction due to the coupling to the transverse current is also neglected for simplicity. The MCT required equilibrium structural information functions of polymer nanocomposites are obtained by using the polymer reference interaction site model (PRISM) theory with Percus-Yevick (PY) closure based on a freely jointed chain (FJC) of polymer.

In this work, we describe our model and theory, and introduce a generalized Langevin equation to describe the diffusion of nanoparticles. A mode-coupling theory is given for evaluating the memory kernel of friction. In addition, PRISM theory is revisited to calculate the equilibrium structural information functions of polymer nanocomposites. In particular, the effect of the nanoparticle size and polymer size will be respectively addressed in detail.

II. MODEL AND THEORY

The diffusion of a free nanoparticle of mass M_n in polymer melts can be conveniently described by a generalized (non-Markov) Langevin equation as follows,

$$\ddot{x}(t) = -\int_0^t \zeta(t-\tau)\dot{x}(\tau)\mathrm{d}\tau + \frac{1}{M_n}\theta(t) \tag{1}$$

where $x(t)$ is the displacement of the particle, $\theta(t)$ is the random force that corresponds to the effects of the thermal fluctuations in polymer solutions, $\zeta(t)$ is the memory kernel of friction. It links to the random force $\theta(t)$ through the fluctuation-dissipation theorem [18],

$$\langle\theta(t)\theta(\tau)\rangle = k_\mathrm{B}TM_n\zeta(t-\tau) \tag{2}$$

where T is the temperature, k_B is the Boltzmann constant.

In order to evaluate the time-dependent diffusion coefficient of nanoparticle, which is defined as [19, 20],

$$D(t) \equiv \frac{1}{2}\frac{\mathrm{d}\langle x^2(t)\rangle}{\mathrm{d}t} \tag{3}$$

we introduce $\tilde{\xi}(s)$ (or $\xi(t)$) as,

$$\tilde{\xi}(s) = \frac{1}{s+\tilde{\zeta}(s)}, \quad \xi(t=0)=1 \tag{4}$$

where $\tilde{}$ denotes the Laplace transformation. $D(t)$ is proven to obey the following expression [9],

$$\begin{aligned} D(t) &= \frac{k_\mathrm{B}T}{M_n}\mathcal{L}^{-1}\left\{\frac{1}{s[s+\tilde{\zeta}(s)]}\right\} \\ &= \int_0^t \frac{k_\mathrm{B}T}{M_n}\xi(\tau)\mathrm{d}\tau \end{aligned} \tag{5}$$

which is wholly determined by the function $\xi(t)$, given by an inverse Laplace transformation of Eq.(4) in terms of friction kernel $\tilde{\zeta}(s)$.

In addition, another central quantity of interest in this work is the conventional diffusion constant D, which is obtained from [8, 6]:

$$D = \frac{k_\mathrm{B}T}{M_n\zeta_0} \tag{6}$$

where ζ_0 is the total time integral of time-dependent friction $\zeta(t)$:

$$\zeta_0 = \int_0^\infty \mathrm{d}t\zeta(t) \tag{7}$$

It is exactly the zero-frequency value of the frequency-dependent friction:

$$\tilde{\zeta}(s=0) = \int_0^\infty \mathrm{d}t\zeta(t) \tag{8}$$

Note that $D(t)$ coincides asymptotically with D as $t\rightarrow\infty$. Indeed, we can observe such a coincidence in the specific results.

The conventional diffusion constant can be also predicated by the classis hydrodynamic Stokes-Einstein (SE) relation [6],

$$D^\mathrm{SE} = \frac{1}{f\pi\eta\sigma_{12}} \tag{9}$$

where $\sigma_{12}=R_n+\sigma/2$ is the cross radius of the monomer-nanoparticle, and f is a constant, which is assumed to

DOI:10.1063/1674-0068/26/02/163-171

be f=6 in the present work corresponding to a stick hydrodynamic boundary condition. η is the shear viscosity coefficient. The diffusion coefficient determined by SE relation is very close to the hydrodynamic limit. The breakdown of the SE law has been extensively discussed in MD calculation and other theoretical works [6, 10, 11].

A. MCT for memory kernel of friction

The memory kernel of friction in polymer melts has been derived previously using the mode-coupling theory [8, 10, 16]. In general, there exist three sources of the friction: binary collision, coupling to the density fluctuation and coupling to the transverse current. The binary collision dominates the short time range of the friction kernel and decays relatively fast. The coupling to the density is responsible to the cage effect and has a long-time memory comparable to the decay of the solvent cage. The coupling to the transverse current refers to the backflow effect where the motion of the tagged particle is coupled with the natural current of the solvent. The former two sources are microscopic contributions, while the last one is due to the hydrodynamic effect. For simplicity, we limit ourselves to analyze the friction arising from the microscopic sources only. The coupling to the transverse current will be neglected in the present work.

Accordingly, the memory kernel of friction $\zeta(t)$ is represented as a sum of two terms: the friction due to the binary collision denoted by $\zeta_b(t)$ and that due to the coupling to the density fluctuation denoted by $\zeta_\rho(t)$, *i.e.*,

$$\zeta(t) = \zeta_b(t) + \zeta_\rho(t) \tag{10}$$

$\zeta_b(t)$ can be approximated by a Gaussian function,

$$\zeta_b(t) = {\omega_b}^2 \exp\left(-\frac{t^2}{{\tau_b}^2}\right) \tag{11}$$

where ω_b is the Einstein frequency and τ_b is the relaxation time. ${\omega_b}^2$ is the initial time value of $\zeta_b(t)$, given by [16]

$$ {\omega_b}^2 = \frac{4\pi\rho_p}{3M_n}\int_0^\infty \mathrm{d}r r^2 g_{np}(r)\nabla^2\phi_{np}(r) \tag{12}$$

with ρ_p being the segment number density, $g_{np}(r)$ and $\phi_{np}(r)$ being the nanoparticle-polymer radial distribution function and interaction potential, τ_b is related to the second-order time derivative of $\zeta_b(t)$ evaluated at initial time. Its microscopic expression is rather lengthy and will not be reproduced here. Details can be found in Ref.[9].

In addition, The MCT result for $\zeta_\rho(t)$ reads [8, 16],

$$\begin{aligned}\zeta_\rho(t) \;=\; & \frac{k_\mathrm{B}T\rho_p}{6\pi^2 M_n N}\int_0^\infty \mathrm{d}k k^4 \hat{C}_{np}(k)^2 F(k,t)\cdot \\ & [F_s(k,t) - F_{s0}(k,t)]\end{aligned} \tag{13}$$

where k is the wave number, N is the segment number of a polymer chain, $\hat{C}_{np}(k)$ is the Fourier transformation of the nanoparticle-polymer direct correlation function. Moreover, $F(k,t)$ is the intermediate scattering function of the chains, which can be obtained in the hydrodynamic approximation,

$$F(k,t) = \exp\left[-\frac{k_\mathrm{B}Tk^2t}{6\pi\eta R_g S(k)}\right] \tag{14}$$

where R_g is the radius of gyration of the polymer chain, and $S(k)$ is the static structure factor of polymer solution. $F_s(k,t)$ is the self-intermediate scattering function of the nanoparticle. We adopt a simple Gaussian model [8, 16],

$$F_s(k,t) = \exp\left\{-\frac{k_\mathrm{B}Tk^2}{M_n\zeta_0}\left[t + \frac{\exp(-t\zeta_0)-1}{\zeta_0}\right]\right\} \tag{15}$$

where ζ_0 is defined in Eq.(7). Note that since Eq.(15) includes ζ_0 and is utilized to determine $\zeta(t)$, ζ_0 should be determined self-consistently. For $F_{s0}(k,t)$, it is the short time inertial limit of $F_s(k,t)$, following

$$F_{s0}(k,t) = \exp\left(-\frac{k_\mathrm{B}Tk^2t^2}{2M_n}\right) \tag{16}$$

B. PRISM for the structural information functions

In order to compute the memory kernel of friction from Eqs.(10)−(13), one needs to know the nanoparticle-polymer radial distribution function and direct correlation function, as well as static structure of the polymer solutions. We obtain these structural quantities from the PRISM theory with PY closure, which has been shown to provide accurate structural information for polymer nanocomposites [21, 22]. PRISM theory is developed by Schweizer and Curro [23, 24] on the basis of the reference interaction site model (RISM) theory [25, 26]. The structural information in this approach is contained in the generalized Ornstein-Zernike (OZ) matric integral equation [26]. In a infinitely dilute nanoparticle limit, OZ relation can be reduced to two uncoupled integral equations for a polymer (p)-nanoparticle (n) system. In Fourier frequency space, it reads [27]

$$\hat{h}_{pp}(k) = \hat{\omega}_p^2(k)\hat{C}_{pp}(k) + \rho_p\hat{\omega}_p(k)\hat{C}_{pp}(k)\hat{h}_{pp}(k) \tag{17}$$

$$\hat{h}_{np}(k) = \hat{\omega}_p(k)\hat{C}_{np}(k) + \rho_p\hat{C}_{np}(k)\hat{h}_{pp}(k) \tag{18}$$

where $h_{ij}(r)$=$g_{ij}(r)$−1 is the intermolecular site-site total correlation function, with $g_{ij}(r)$ being the intermolecular pair correlation function. $C_{ij}(r)$ is the corresponding intermolecular direct correlation function, and $\hat{\omega}_p(k)$ is the structure factor of single polymer.

The polymer is treated as a freely jointed chain (FJC) of N monomers, with the same site diameter σ and mass

DOI:10.1063/1674-0068/26/02/163-171

m, and a rigid bond length l=1.269σ [27]. The structure factor for FJC is [28, 29]

$$\hat{\omega}_p(k) = \frac{1 - f^2 - 2f/N + 2f^{N+1}/N}{(1-f)^2} \quad (19)$$

where f=sin(kl)/kl. The nonideal conformation effect ignored by the FJC model is minor for the melt conditions.

With the prescribed $\hat{\omega}_p(k)$ in Eq.(19), closure approximation must be employed to uniquely determine $h_{ij}(r)$ and $C_{ij}(r)$ from Eq.(17) and Eq.(18). The site-site PY approximation [26, 30] is adopted for the polymer-polymer and nanoparticle-polymer direct correlations,

$$C_{ij}(r) \cong g_{ij}(r)\left\{1 - \exp\left[\frac{\phi_{ij}(r)}{k_\mathrm{B}T}\right]\right\} \quad (20)$$

where $\phi_{ij}(r)$ is the total site-site interaction potential. The site-site PY closure has been shown to be accurate for pure polymers and nanoparticle-polymer correlations under dense melt conditions [23, 24, 31, 32]. The interactions between monomers are described via LJ potential, truncated and shifted at its minimum:

$$\phi_{pp}(r) = \begin{cases} 4\epsilon\left[\left(\dfrac{\sigma}{r}\right)^{12} - \left(\dfrac{\sigma}{r}\right)^{6} + \dfrac{1}{4}\right], & (r < 2^{1/6}\sigma) \\ 0, & (r \geq 2^{1/6}\sigma) \end{cases} \quad (21)$$

where ϵ is the potential well depth. The nanoparticles are modeled as LJ spheres of radius R_n and mass M_n. The interactions between nanoparticle and polymer segment are described via LJ potential which is offset by the interaction range R_EV=R_n−σ/2:

$$\phi_{np}(r) = \begin{cases} 4\epsilon_{np}\left[\left(\dfrac{\sigma}{r - R_\mathrm{EV}}\right)^{12} - \left(\dfrac{\sigma}{r - R_\mathrm{EV}}\right)^{6}\right], \\ \qquad\qquad r > R_\mathrm{EV} \\ \infty, \qquad\quad r \leq R_\mathrm{EV} \end{cases} \quad (22)$$

The potential is truncated and shifted at the separation r_{np}^cut=R_EV+2.5σ. For simplicity, we assume identical interaction strength ϵ_{np}=ϵ throughout this work.

Combining Eqs.(19)−(22) and the OZ relation Eq.(17) and Eq.(18), we have a closed equation system to determine the structural functions for polymer nanocomposites, including $g_{pp}(r)$, $C_{pp}(r)$, $g_{np}(r)$, and $C_{np}(r)$. The iterative Picard method is utilized to solve the integral equations [30].

Finally, the polymer-polymer partial collective structure factor can be obtained from

$$\hat{S}_{pp}(k) = \hat{\omega}_p(k) + \rho\hat{h}_{pp}(k) \quad (23)$$

The static (center of mass) structure factor $S(k)$ is therefore [33]

$$S(k) = \frac{\hat{S}_{pp}(k)}{\hat{\omega}_p(k)} \quad (24)$$

TABLE I The gyration radius R_g^* and shear viscosity coefficient η^* of polymer, as well as the intermediate calculated parameters ω_b^{*2}, τ_b^* and ζ_0^* for varying N. R_n^* = 0.5 and M_n^*=1 are fixed.

N	R_g^*	η^*	ω_b^{*2}	τ_b^*	ζ_0^*
10	1.487	7.09	268.114	0.0670	92.468
20	2.157	12.1	244.809	0.0669	44.928
30	2.753	20.7	233.785	0.0667	25.516
40	3.226	33.8	227.107	0.0666	19.380
60	4.028	42.5	219.165	0.0664	15.526
80	4.682	53.6	214.459	0.0663	14.208
120	5.925	130	208.947	0.0662	13.118

III. SPECIFIC RESULTS

Based on the theoretical formalism, we proceed to evaluate the specific numerical results for the equilibrium structural information functions, the friction kernel, and the resulting time-dependent diffusion coefficient and conventional diffusion constant. The effect of the nanoparticle size and that of the polymer size (polymer chain length scale) will be elaborated particularly. Our results will be presented in terms of dimensionless quantities defined as follows,

$$\rho^* \equiv \rho\sigma^3,\quad T^* \equiv \frac{k_\mathrm{B}T}{\epsilon},\quad R_n^* \equiv \frac{R_n}{\sigma},\quad R_g^* \equiv \frac{R_g}{\sigma},$$
$$r^* = \frac{r}{\sigma},\quad k^* = k\sigma,\quad M_n^* \equiv \frac{M_n}{m},\quad t^* \equiv \frac{t}{\sqrt{m\sigma^2/\epsilon}},$$
$$\zeta^* \equiv \frac{\zeta\epsilon}{m\sigma^2},\quad \eta^* \equiv \frac{\eta\sigma}{\sqrt{m\epsilon}},\quad D^* \equiv D\sqrt{\frac{m}{\epsilon\sigma^2}}$$

In the calculation, we fix the number density of monomers of the polymer at ρ_p^*=0.84 and the temperature of the solution T^*=1. The nanoparticle varies the mass with its radius according to M_n^*=8R_n^{*3}, *i.e.*, the mass of the nanoparticle is taken to be proportional to its volume, with the mass density of nanoparticle taken to be the same as that of monomers [6]. The effect of nanoparticle size will be investigated by varying the nanoparticle radius from R_n^*=0.5 to R_n^*=3.0, with fixed polymer chain length at N=80. Moreover, the polymer size effect will be analyzed by increasing the polymer chain length from N=10 to N=120 with fixed nanoparticle radius at R_n^*=0.5. In the calculation, the polymer radius of gyration R_g^* and the shear viscosity coefficient η^* of the polymer melt are adopted according to the MD simulation [6, 34, 35], see Table I.

A. The effect of nanoparticle size

We start to study the effect of nanoparticle size. To this end, we gradually increase the nanoparticle radius R_n^*, while keeping the polymer chain length fixed at

DOI:10.1063/1674-0068/26/02/163-171

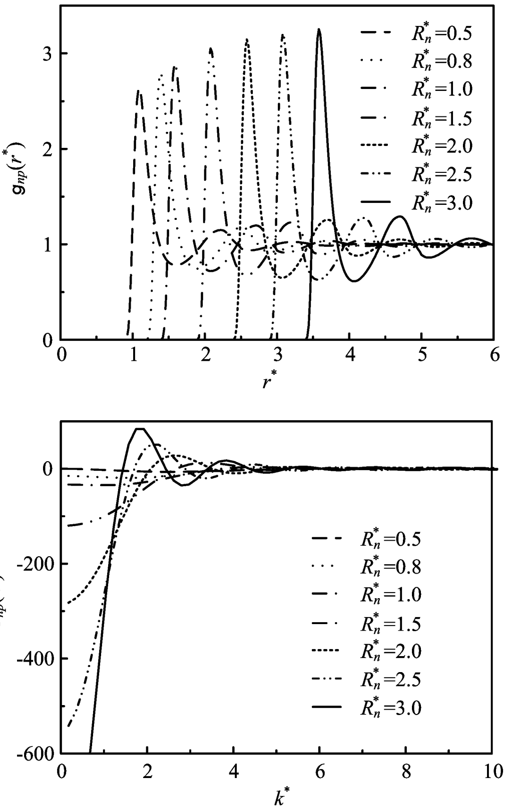

FIG. 1 The nanoparticle-polymer radial distribution function $g_{np}(r^*)$ and direct correlation function $\hat{C}_{np}(k)$, for varying nanoparticle size but fixed polymer chain length at N=80.

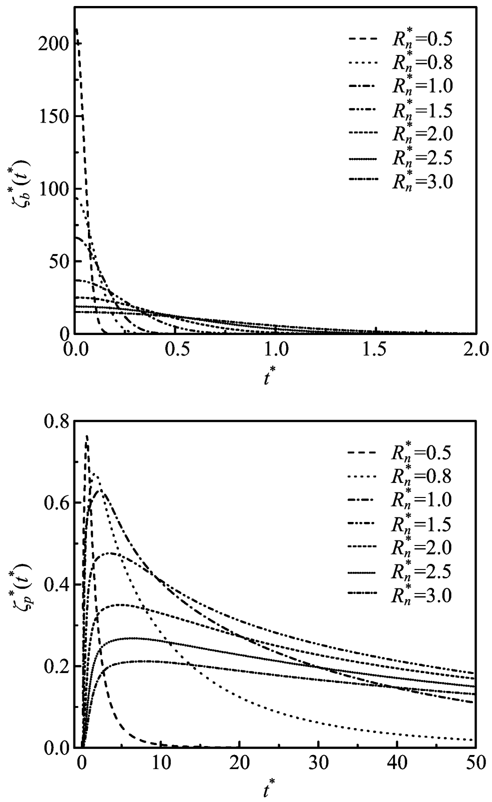

FIG. 2 The time-dependent friction term due to the binary collision $\zeta_b^*(t^*)$ and that due to the coupling to the density fluctuation $\zeta_\rho^*(t^*)$, for varying nanoparticle size but fixed polymer chain length at N=80.

N=80. Using the PRISM theory, the required equilibrium structural functions of polymer, including the radial distribution function $g_{pp}(r^*)$ and static structure factor $S(k^*)$, are obtained, to be independent of the nanoparticle radius R_n^*. Simultaneously, we obtain the nanoparticle-polymer radial correlation function $g_{np}(r^*)$ and the direct correlation function $\hat{C}_{np}(k^*)$. Figure 1 shows the $g_{np}(r^*)$ and $\hat{C}_{np}(k^*)$ for nanoparticle size varying from R_n^*=0.5 to R_n^*=3.0. It can be seen from this figure that as R_n^* increases, $g_{np}(r^*)$ shifts towards right, and the intensity of its peak is slightly strengthened. In addition, $\hat{C}_{np}(k^*)$ exhibits an oscillatory behavior which becomes stronger with the increase of R_n^*.

Using these functions, the memory kernel of friction can be calculated subsequently. With Eqs. (11)−(13), we obtain the friction due to the binary collision $\zeta_b^*(t^*)$ and that due to the coupling to the density fluctuation $\zeta_\rho^*(t^*)$, as shown in Fig.2. The relevant calculated parameters are listed in Table II. It can be seen that $\zeta_b^*(t^*)$ dominates the friction in short time regime, while $\zeta_\rho^*(t^*)$ determines the behavior over long time period. As R_n^* increases, the initial value of $\zeta_b^*(t^*)$ (*i.e.*, ${\omega_b^*}^2$) and the intensity of the peak of $\zeta_\rho^*(t^*)$ decreases, while both of them undergo an extended relaxation time. Figure 3

TABLE II The intermediate calculated parameters M_n^*, ${\omega_b^*}^2(\equiv \omega_b^2\epsilon/m\sigma^2)$, $\tau_b^*(\equiv \tau_b/\sqrt{m\sigma^2/\epsilon})$, and ζ_0^* for varying R_n^*. N=80 is fixed. R_g^*=4.682 and η^*=53.6 according to Table I.

R_n^*	M_n^*	${\omega_b^*}^2$	τ_b^*	ζ_0^*
0.5	1	214.459	0.0663	14.208
0.8	4.096	93.995	0.134	19.750
1.0	8	66.497	0.187	29.269
1.5	27	36.955	0.320	39.901
2.0	64	25.109	0.427	39.503
2.5	125	18.885	0.492	37.403
3	216	15.087	0.525	35.199

displays the total friction $\zeta^*(t^*)$ as a combination of $\zeta_b^*(t^*)$ and $\zeta_\rho^*(t^*)$ for several values of R_n^*. A clear bimodality is demonstrated, which is particularly prominent for small nanoparticles. For large nanoparticles, this friction is more likely a monotonous decay in the overall time period.

Furthermore, we calculate the time-dependent diffusion coefficient $D^*(t^*)$ based on Eq.(5). Inserting the numerical results of friction kernel $\zeta^*(t^*)$ just obtained above, after integral we plot immediately Fig.4. As it is shown, $D^*(t^*)$ firstly experiences a sharp initial raise to

DOI:10.1063/1674-0068/26/02/163-171

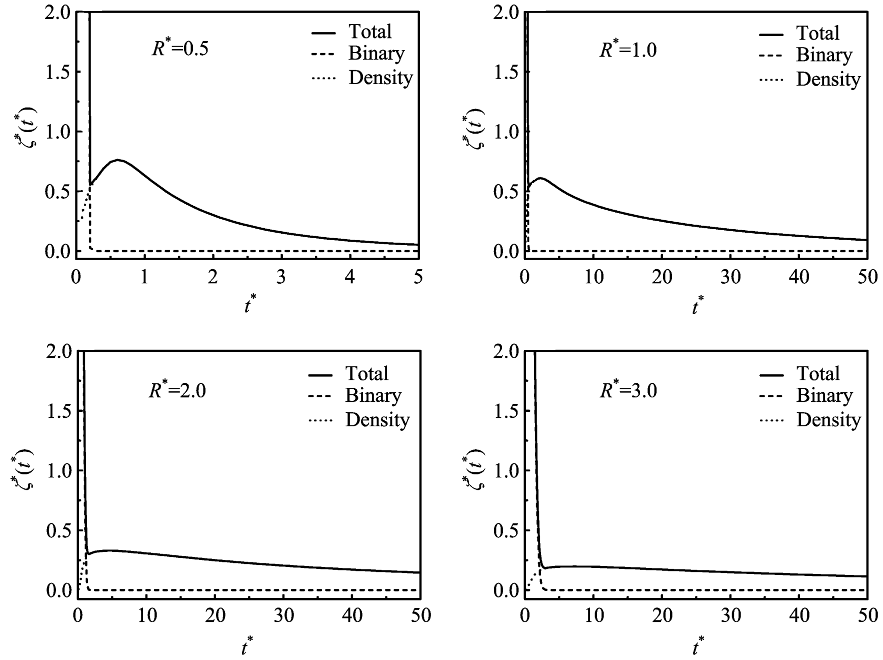

FIG. 3 The time-dependent total friction kernel $\zeta^*(t^*)$ as a combination of binary term $\zeta_b^*(t^*)$ and density fluctuation term $\zeta_\rho^*(t^*)$, for R_n^*=0.5, 1.0, 2.0, 3.0. Polymer size is fixed at N=80.

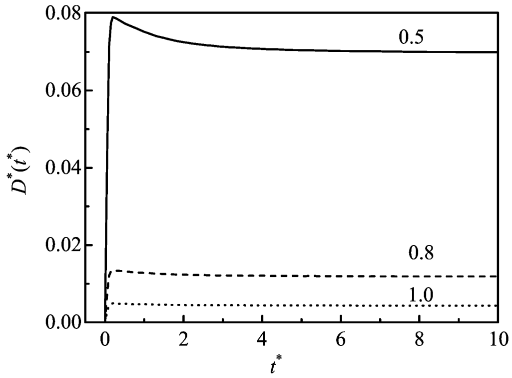

FIG. 4 The time-dependent diffusion coefficient $D^*(t^*)$ for R_n^*=0.5, 0.8, and 1.0, at common polymer size N=80.

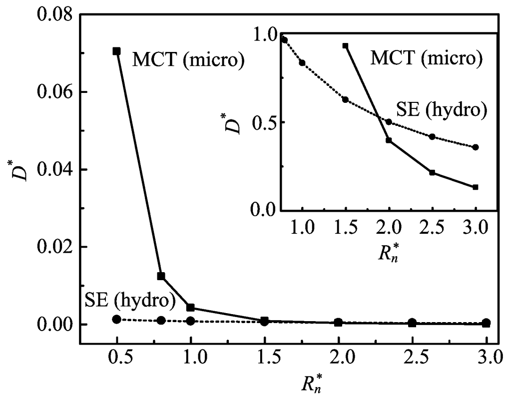

FIG. 5 The nanoparticle size R_n^* dependence of the microscopic part of diffusion constant D^* obtained from MCT and the hydrodynamic part predicted from SE relation. The polymer size is fixed at N=80.

a maximum, then it decays little and finally reaches its long-time asymptotic value D_∞^*. As R_n^* increases, this value decreases rapidly. The time-dependent diffusion behavior in short time regime is evident, in particular, for small nanoparticles. Although, this transient dynamics occurs over a relatively narrow time period, not as broad as that of particles in simple liquids [9], it brings about a non-Markov nature of the diffusion dynamics in a certain degree.

Finally, by aid of Eq.(6) and Eq.(7), we evaluate the conventional diffusion constant. Note that the zero-frequency friction ζ_0^* as well as the total time integral of $\zeta^*(t^*)$ is just the value presented in Table II which is self-consistently determined in the calculation of the friction kernel. The resultant D^* is plotted in Fig.5, which obviously coincides with the long-time asymptotic value D_∞^* as shown in Fig.4. With the increase of R_n, this coefficient decreases fast. Meanwhile, the value predicted from SE relation is also displayed for comparison. Note here that the diffusion constant from the standpoint of the present MCT formalism only includes the microscopic sources, *i.e.*, the binary collision and the coupling to the density fluctuation. The SE relation, however, is a good approximation for hydrodynamic contribution. Clearly, for small nanoparticles (*e.g.*, R_n^*<0.8), D^* from MCT exceeds the SE-predicted value by up to an order of magnitude. It means in this nanoparticle size regime, the diffusion is largely domi-

DOI:10.1063/1674-0068/26/02/163-171

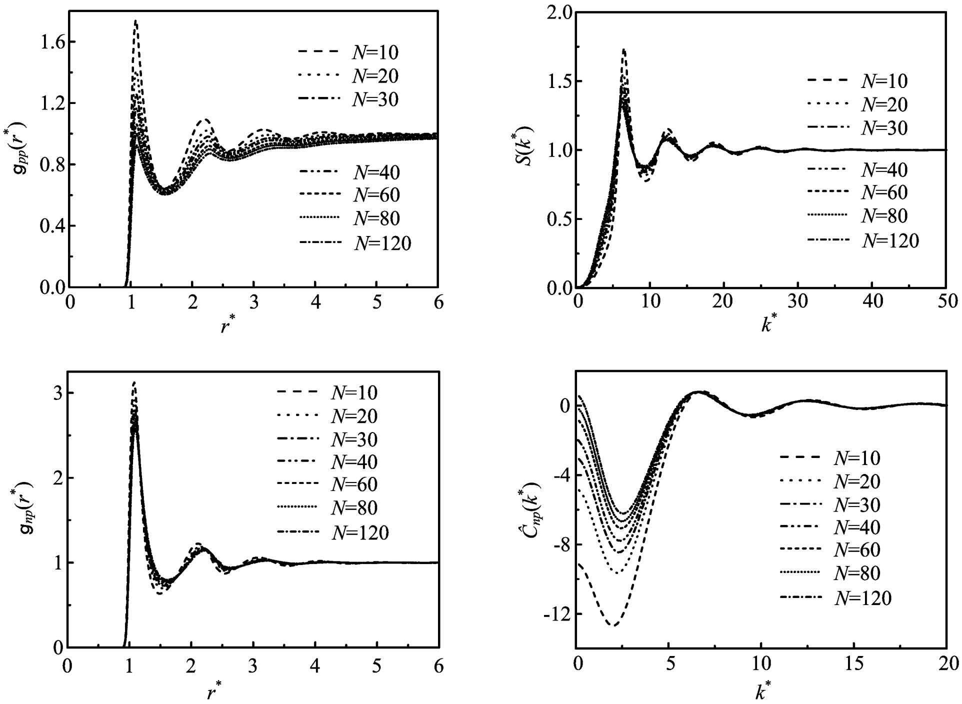

FIG. 6 The polymer-polymer radial distribution function $g_{pp}(r^*)$, the static structure factor $S(k^*)$ of polymer melts, the nanoparticle-polymer radial distribution function $g_{np}(r^*)$ as well as direct correlation function $\hat{C}_{np}(k^*)$, for varying polymer size but fixed nanoparticle radius at R_n^*=0.5.

nated by the microscopic contribution. The same qualitative behavior has been observed in an earlier MCT study of anomalous diffusion of small solutes in simple dense liquids [8], and that of nanoparticles in polymer solutions based on Gaussian chain model calculation [10]. As the nanoparticle radius is gradually increased, both microscopic and hydrodynamic terms give comparable contributions to the total diffusion coefficient. For large nanoparticles (*e.g.*, R_n^*>2.0), the diffusion coefficient is conversely dominated by the hydrodynamic SE relation. As such, the diffusion coefficient in this regime is inversely proportional to the nanoparticle radius.

B. The effect of polymer size

We now vary the polymer chain length from N=10 to N=120 in order to analyze the effect of polymer size on the equilibrium structural functions, the friction kernel as well as the nanoparticle diffusion coefficient. The gyration radius R_g^* and shear viscosity coefficient η^* vary their value with the polymer size according to Table I. The nanoparticle size is fixed at R_n^*=0.5, so that the mass of the nanoparticle keeps to be M_n^*=1. As a result of PRISM theory, we obtain simultaneously the solutions of the radial distribution function $g_{pp}(r^*)$ and static structure factor $S(k^*)$ for polymer solutions, and those of the nanoparticle-polymer radial distribution function $g_{np}(r^*)$ and direct correlation function $\hat{C}_{np}(k^*)$. Figure 6 shows the resultant curves for various polymer length scales. As demonstrated, all curves exhibit clear oscillatory behavior, where the intensity of the first peak decreases with the increase of polymer size, while the location of the peak is kept.

The friction kernel due to binary collision $\zeta_b^*(t^*)$ and that due to the coupling to the density fluctuation $\zeta_\rho^*(t^*)$ are also obtained, shown in Fig.7. The intermediate calculated parameters are listed in Table I. It's evident that as N increases, the initial value of $\zeta_b^*(t^*)$ (*i.e.* ${\omega_b^*}^2$) and the amplitude of $\zeta_\rho^*(t^*)$ decrease. Their relaxation time, however, are almost unaltered with the polymer size. This feature results in the monotonous decrease of the zero-frequency of friction ζ_0^* with the increase of N (see the corresponding data in Table I), and thus the monotonous decrease of diffusion coefficient D^*. The final result of the total time-dependent friction $\zeta^*(t^*)$ is easily obtained as a combination of these two terms, and is omitted here for simplicity. We find a bimodality behavior similar to Fig.3.

At last, the time-dependent diffusion coefficient $D^*(t^*)$ for N=10, 20, 30 is displayed in Fig.8. We see that the time-dependent diffusion coefficient firstly experiences an oscillation and then approaches D_∞^* gradually. The oscillatory behavior likely reduces to a smooth decay as the polymer size increases. For shorter polymer, the diffusion coefficient takes longer time to approach asymptotically the conventional diffusion constant. As mentioned above, this transient dynamics is

DOI:10.1063/1674-0068/26/02/163-171

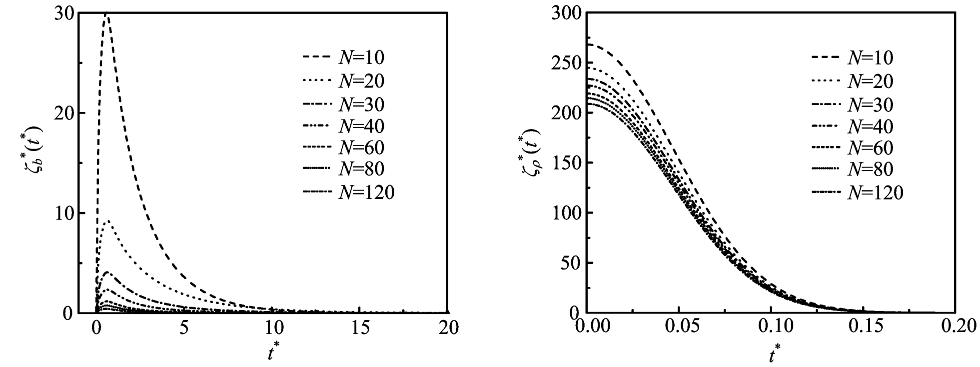

FIG. 7 The time-dependent friction term due to the binary collision $\zeta_b^*(t^*)$ and that due to the coupling to the density fluctuation $\zeta_\rho^*(t^*)$, for varying polymer size but fixed nanoparticle radius at R_n^*=0.5.

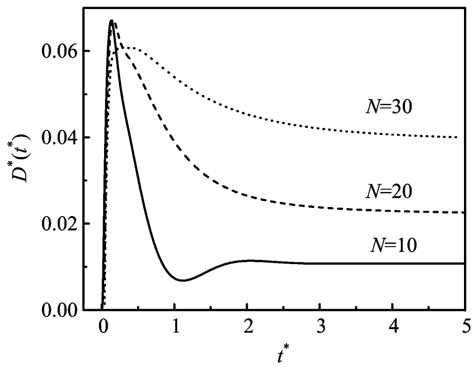

FIG. 8 The time-dependent diffusion coefficient $D^*(t^*)$ for N=10, 20, 30, at common nanoparticle radius R_n^*=0.5.

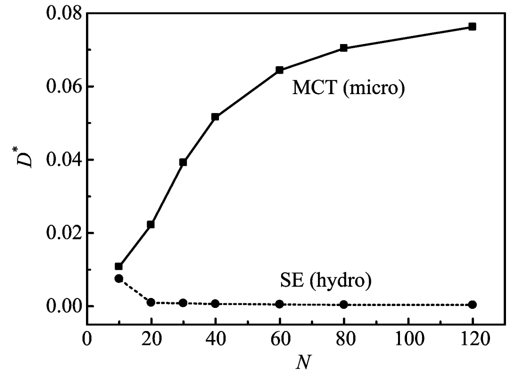

FIG. 9 The polymer size N dependence of the microscopic part of diffusion constant D^* obtained from MCT and the hydrodynamic part predicted from SE relation. The nanoparticle radius is fixed at R_n^*=0.5.

very important for the study of the non-Markov nature of the diffusion dynamics. The long-time asymptotic value D_∞^* shown in Fig.8 increases with the increase of polymer size. Furthermore, we calculate the conventional diffusion constant D^* using Eq.(6) directly. This value is proven to be quantitatively in agreement with the asymptotic value D_∞^* in Fig.8. Again, we note that D^* obtained here is based on a simplified framework of MCT where only microscopic contributions are taken into account.

Figure 9 presents D^* from MCT and that from SE relation Eq.(7). Evidently, for short chains (*e.g.*, $N<20$), two results are in the same order of magnitude, implying both microscopic and hydrodynamic contributions play a comparable role in the diffusion dynamics. Nevertheless, for long chains, (*e.g.*, $N>20$), the MCT result is almost dominant, exceeding the hydrodynamic contribution up to an order of magnitude. In such a polymer size regime, the hydrodynamic contribution to diffusion might be negligible.

IV. CONCLUSION

In this work, we apply GLE to study diffusion dynamics of nanoparticles in polymer melts, where the friction kernel is calculated from MCT formalism, including only two microscopic terms respectively due to binary collision and the coupling to the density fluctuation. The equilibrium structural information functions of polymer nanocomposites required by MCT are obtained from PRISM theory with PY closure. Not only the usual diffusion constant but also the time-dependent diffusion coefficient is explicitly analyzed. Besides, the effect of the nanoparticle size and that of the polymer size are particularly explored. The equilibrium structural information functions of polymer nanocomposites, the memory kernel of friction, and the diffusion coefficient exhibit a rich variety with varying nanoparticle size and polymer chain length. Furthermore, the conventional diffusion constant from MCT is compared with the value predicted from the SE relation. It shows, for small nanoparticles or long chain polymer, the microscopic contributions dominate the diffusion dynamics. In contrast, for large nanoparticles or short chain polymer, the hydrodynamic contribution approximated by SE relation plays a significant role.

It should be emphasized that compared with the previous studies of the diffusion of nanoparticles in polymer melts where only conventional diffusion constant is investigated, our work deals with both the time-dependent diffusion coefficient and the conventional diffusion constant. This provides an overall picture of the diffusion behavior of nanoparticles in polymer melts, facilitating understanding the non-Markov nature in the associated dynamics. We should note that the present work is limited to the microscopic origins of friction kernel, where the hydrodynamic contribution due to the coupling to the transverse current is omitted. Moreover, the entanglement effect of the polymer chain is also neglected in the present study. Further study of diffusion dynamics of nanoparticles in unentangled and entangled polymer melts based on a complete version of MCT including both microscopic and hydrodynamic terms is quite desirable. This will be the task of our forthcoming paper.

V. ACKNOWLEDGMENTS

This work was supported by the National Natural Science Foundation of China (No.21173152), the Ministry of Education of China (No.NCET-11-0359 and No.2011SCU04B31), and the Science and Technology Department of Sichuan Province (No.2011HH0005).

[1] H. J. Lin, H. Y. Chen, Y. J. Sheng, and H. K. Tsao, Phys. Rev. Lett. **98**, 088304 (2007).
[2] M. Schlierf, H. B. Li, and J. M. Fernandez, Proc. Natl. Acad. Sci. USA **101**, 7299 (2004).
[3] O. K. Dudko, J. Mathe, A. Szabo, A. Meller, and G. Hummer, Biophys. J. **92**, 4188 (2007).
[4] D. L. Hunter, K. W. Kamena, and D. R. Paul, MRS Bull. **32**, 323 (2007).
[5] J. Liu, L. Zhang, D. Cao, and W. Wang, Phys. Chem. Chem. Phys. **11**, 11365 (2009).
[6] J. Liu, D. Cao, and L. Zhang, J. Phys. Chem. C **112**, 6653 (2008).
[7] C. A. Grabowski, B. Adhikary, and A. Mukhopadhyay, Appl. Phys. Lett. **94**, 021903 (2009).
[8] S. Bhattacharyya and B. Bagchi, J. Chem. Phys. **106**, 1757 (1997).
[9] A. Morita and B. Bagchi, J. Chem. Phys. **110**, 8643 (1999).
[10] S. A. Egorov, J. Chem. Phys. **134**, 084903 (2011).
[11] U. Yamamoto and K. S. Schweizer, J. Chem. Phys. **135**, 224902 (2011).
[12] M. Praprotnik, L. D. Site, and K. Kremer, J. Chem. Phys. **126**, 134902 (2007).
[13] I. Kohli and A. Mukhopadhyay, Macromolecules **45**, 6143 (2012).
[14] V. Ganesan, V. Pryamitsyn, M. Surve, and B. Narayanan, J. Chem. Phys. **124**, 221102 (2006).
[15] M. Kruger and M. Rauscher, J. Chem. Phys. **131**, 094902 (2009).
[16] U. Balucani and M. Zoppi, *Dynamics of the Liquid State*, New York: Oxford University Press. (1994).
[17] B. Bagchi and S. Bhattacharyya, Adv. Chem. Phys. **116**, 67 (2001).
[18] R. Kubo, Rep. Prog. Phys. **29**, 255 (1966).
[19] R. Morgado, F. A. Oliveira, G. G. Batrouni, and A. Hansen, Phys. Rev. Lett. **89**, 100601 (2002).
[20] Y. X. Wang, N. R. Zhao, and Y. J. Yan, Phy. Rev. E **85**, 041142 (2012).
[21] A. P. Chatterjee and K. S. Schweizer, J. Chem. Phys. **109**, 10464 (1998).
[22] A. P. Chatterjee and K. S. Schweizer, J. Chem. Phys. **109**, 10477 (1998).
[23] K. S. Schweizer and J. G. Curro, Adv. Polym. Sci. **116**, 321 (1994).
[24] K. S. Schweizer and J. G. Curro, Adv. Chem. Phys. **98**, 1 (1997).
[25] D. Chandler and H. C. Andersen, J. Chem. Phys. **57**, 1930 (1972).
[26] D. Chandler, *Studies in Statistical Mechanics VIII*, E. W. Montroll and J. L. Lebowitz, Eds., Amsterdam: North-Holland, 274 (1982).
[27] L. Zhao, Y. Li, C. Zhong, and J. Mi, J. Chem. Phys. **124**, 144913 (2006).
[28] J. G. Curro, K. S. Schweizer, G. S. Grest, and K. Kremer, J. Chem. Phys. **91**, 1357 (1989).
[29] M. Doi and S. F. Edwards, *Theory of Polymer Dynamics*, New York: Oxford University Press, (1986).
[30] J. P. Hansen and I. R. McDonald, *Theory of Simple Liquids*, 2nd Edn., London: Academic, (1986).
[31] M. Doxastakis, Y. L. Chen, O. Guzman, and J. J. de Pablo, J. Chem. Phys. **120**, 9335 (2004).
[32] N. Patel and S. A. Egorov, J. Chem. Phys. **121**, 4987 (2004).
[33] K. Miyazaki, B. Bagchi, and A. Yethiraj, J. Chem. Phys. **121**, 8120 (2004).
[34] M. Kroger, W. Loose, and S. Hess, J. Rheol. **37**, 1057 (1993).
[35] S. Sen, S. K. Kumar, and P. Keblinski, Macromolecules **38**, 650 (2005).

DOI:10.1063/1674-0068/26/02/163-171